Nanoscale Res Lett (2010) 5:1633–1636
DOI 10.1007/s11671-010-9687-x

NANO EXPRESS

Single-dot Spectroscopy of GaAs Quantum Dots Fabricated by Filling of Self-assembled Nanoholes

Ch. Heyn · M. Klingbeil · Ch. Strelow · A. Stemmann · S. Mendach · W. Hansen

Received: 15 June 2010 / Accepted: 1 July 2010 / Published online: 14 July 2010

Abstract We study the optical emission of single GaAs quantum dots (QDs). The QDs are fabricated by filling of nanoholes in AlGaAs and AlAs which are generated in a self-assembled fashion by local droplet etching with Al droplets. Using suitable process parameters, we create either uniform QDs in partially filled deep holes or QDs with very broad size distribution in completely filled shallow holes. Micro photoluminescence measurements of single QDs of both types establish sharp excitonic peaks. We measure a fine-structure splitting in the range of 22–40μeV and no dependence on QD size. Furthermore, we find a decrease in exciton–biexciton splitting with increasing QD size.

Introduction

Semiconductor quantum dots (QDs) are very attractive for advanced applications for instance in the field of quantum computing [1] and as single photon sources [2, 3] for quantum cryptography. In this context, the detailed knowledge of the symmetries and level-structure inside these artificial atoms and its correlation to the QD structural properties is essential. A prominent example is the excitonic fine-structure splitting (FSS) which is a crucial parameter for the generation of entangled photons for cryptography [3, 4]. The FSS is related to the exchange interaction between electrons and holes in the strong QD confinement [5–7] and can be measured for instance by using micro photoluminescence (PL) spectroscopy [8, 9].

Most studies on the fine structure in single-dot PL have been performed on self-assembled InAs QDs [7, 9–11] grown on (001) GaAs. The FSS in InAs QDs is caused by at least three different effects: dominantly by the strain-induced piezoelectricity, furthermore, by the QD elongation, and by atomistic anisotropy [7]. Unintentional intermixing with substrate material [12, 13] causes a poorly known QD composition and strain distribution [14], and, thus, significantly complicates studies of the relation between the FSS and the structural properties of the strain-induced QDs.

A more clear situation is found in the case of strain-free GaAs QDs, where piezoelectricity is expected to have negligible contribution. The excitonic fine structure of several types of GaAs QDs has been studied so far [8, 15–17]. First studies have been performed on so-called natural QDs [8]. These are formed by quantum-well interface-fluctuations and have relatively small lateral quantization energies. Larger GaAs QDs have been fabricated with droplet epitaxy [15], or filling of nanoholes which are generated either by pre-patterning with lithography [16] or by in situ gas etching [17].

This work presents results on the excitonic fine structure of a novel type of strain-free GaAs QDs which are fabricated by filling of self-assembled nanoholes at usual molecular beam epitaxy (MBE) growth temperatures without any lithographic or gas etching steps. The nanoholes are generated in AlGaAs and AlAs surfaces in situ, i.e. during MBE process, using local droplet etching (LDE) [18–23]. Examples are shown in Fig. 1a, b. During LDE, liquid droplets of Ga, In, or Al are deposited on a surface in Volmer–Weber growth mode. The present understanding of the etching mechanism is that during the subsequent

Ch. Heyn (✉) · M. Klingbeil · Ch. Strelow · A. Stemmann · S. Mendach · W. Hansen
Institut für Angewandte Physik und Zentrum für Mikrostrukturforschung, Jungiusstraße 11, D-20355 Hamburg, Germany
e-mail: heyn@physnet.uni-hamburg.de

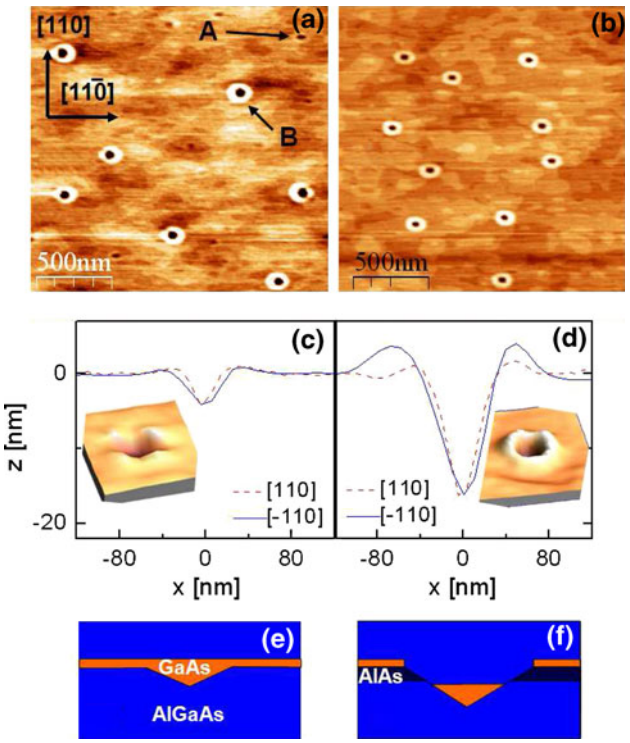

Fig. 1 **a** Top view AFM image of an AlGaAs surface after LDE with Al droplets at $T = 620$°C. *Arrow* "*A*" marks a *shallow hole* and "*B*" a *deep hole*. **b** Top view AFM image of an AlGaAs surface after LDE with Ga droplets at $T = 620$°C. **c** Profile and 3D view of the *shallow hole* "*A*" in (**a**). **d** Profile and 3D view of the *deep hole* "*B*" in (**a**), **e** Schematic cross-section of a *shallow-hole* QD (type I sample). **f** Schematic cross-section of a *deep-hole* QD (type II sample)

annealing step, arsenic from the substrate diffuses into the droplets which causes a liquefaction of the substrate at the interface to the droplet. After desorption of all liquid material, nanoholes are formed and finally filled with GaAs in order to create the QDs.

Sample Preparation

The samples discussed in the following are fabricated using solid-source MBE. After thermal oxide desorption, a 200-nm-thick $Al_{0.35}Ga_{0.65}$ As barrier layer was grown on a (001) GaAs substrate. We have fabricated two types of samples denoted in the following as type I and type II. For the type II samples, an additional 5-nm-thick AlAs layer was grown on top of the AlGaAs layer. Now, the As shutter and valve were closed and Al droplet formation was initiated by opening the Al shutter for 6 s. The temperature was $T = 620$°C for type I and $T = 650$°C for type II samples. The Al flux corresponded to a growth speed of 0.47 ML/s and droplet material was deposited onto the surface with coverage of 2.8 ML. After droplet deposition, a thermal annealing step of 180 s was applied. During this time, the etching process takes place, liquid etching residues are removed, and a wall surrounding the nanoholes is formed [22].

The nanoholes were filled with GaAs at a substrate temperature of $T = 600$°C in a pulsed mode by applying n_P pulses with 0.5 s growth and 30 s pause, respectively. We present results of two type I samples, one with $n_P = 3$ and one with $n_P = 7$, which corresponds to GaAs layers with thickness $d_f = 0.34$ nm and 0.79 nm, respectively. The additional type II sample was filled with $d_f = 0.57$ nm resulting in uniform QDs with height of 7.6 nm [25]. Finally, the QDs were capped by a 120-nm-thick $Al_{0.35}Ga_{0.65}$ As barrier.

Types of GaAs Quantum Dots

Figure 1a shows an atomic force microscopy (AFM) image of the AlGaAs surface of a typical type I sample after Al LDE. Clearly visible on this surface is the coexistence of shallow holes (up to 7 nm depth) and deep holes (deeper than 7 nm). We have already observed this effect earlier for Ga LDE on AlGaAs at low temperatures [20]. On the other hand, type II samples have no such bimodal depth distribution and the resulting surfaces show only deep holes [24, 25]. Since the AlAs surfaces of type II samples oxidate very fast and, thus, are not accessible to AFM measurements under air, for illustration we provide a sample where Ga LDE has been performed on AlGaAs at $T = 620$°C. The corresponding surface (Fig. 1b) shows only deep holes, similar to the type II samples.

These surfaces act as a template for the QD formation by filling of the nanoholes with GaAs. Both types of samples with the different nanoholes result in different types of QDs. The deep nanoholes in type II samples are only partially filled (Fig. 1f) and yield highly uniform QDs with size precisely controlled by the filling level [24]. Photoluminescence (PL) measurements of QD ensembles formed only in deep holes demonstrate extremely narrow linewidths of less then 10 meV [25]. Furthermore, we assume that the deep-hole QDs are not in contact with the GaAs quantum well used for filling.

On the other hand, shallow holes in type I samples are completely filled (Fig. 1e) and the QD size is given by the hole depth with broad distribution [20]. As a consequence, ensembles of shallow-hole QDs show a very broad optical emission band and no systematic influence of the filling level d_f [24]. This provides the interesting advantage that a large range of QD sizes can be studied on a single type I sample. In contrast to the deep-hole QDs, QDs formed in shallow holes are in direct contact with the GaAs quantum well used for filling.

Single-dot Spectroscopy

Single-dot PL spectroscopy was performed using micro PL at $T = 4$ K with a focussed laser for excitation. Examples from a shallow-hole QD and a deep-hole QD are plotted in Fig. 2. Importantly, both types of QDs exhibit sharp excitonic lines. At low excitation power I_e, we find a neutral exciton peak X with full width at half maximum (FWHM) of 180 μeV for the shallow-hole QD and of 60 μeV for the deep-hole QD. With increasing I_e, the biexciton peak XX, charged excitons, and higher excitonic complexes arise. The exciton and biexciton peaks were identified on basis of their excitation power dependence (Fig. 3a), with slope of one for X and of two for XX.

Polarization-dependent measurements of the neutral exciton and biexciton peaks reveal a polarization angle α-dependent shift of the peak maxima that is related to the FSS. The deviation of the peak maxima E from the average peak energy E_{av} is fitted by the expression $E = E_{av} + (\mathrm{FSS}/2)\sin(\alpha_0 + 2\alpha)$. Figures 3b, c show examples with

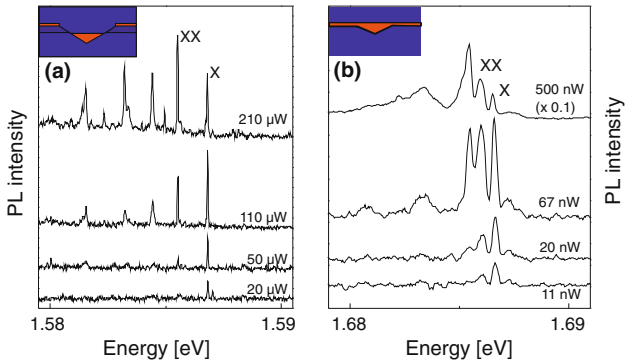

Fig. 2 **a** Micro PL spectra of a single *deep-hole* QD with height of 7.6 nm taken at varied excitation power I_e. **b** Micro PL spectra of a single *shallow-hole* QD at varied I_e. The laser energy is 2.33 eV. The spectra are vertically shifted for clarity. The exciton peaks are labeled as *X* and the biexciton as *XX*

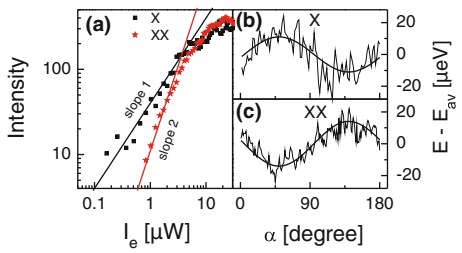

Fig. 3 **a** Symbols: excitation power dependence of the *X* and *XX* peaks of the *shallow-hole* QD of Fig. 2a. Lines: fits with slope = 1 for the *X* and slope = 2 for the *XX* peaks. **b** Position of the *X* peak maximum of the *shallow-hole* QD of Fig. 2a at $I_e = 110$ nW as function of the analyzer polarization angle α together with a fit using a sinus function as described in text. **c** Polarization angle dependent maximum of the *XX* peak with fit. The FSS is 22 μeV for the *X* and 28 μeV for the *XX* peak, respectively

an exciton FSS of 22 μeV and a bieciton splitting of 28 μeV. These data demonstrate the state of the art optical quality of LDE GaAs QDs being comparable to the established InAs dots.

With the above procedure, the FSS of several QDs in two samples with different filling level d_f was determined. We use shallow-hole QDs for these measurements since they allow to analyze QDs with different sizes on one sample. The results are plotted in Fig. 4a as function of the peak energy. We find values of the FSS between 22 and 40 μeV. Importantly, dots from both samples behave very similar indicating complete filling of the shallow holes even at the lower filling level. Excluding the strain-induced piezoelectricity, the occurrence of a FSS in our strain-free GaAs QDs can be caused by the dot elongation [6, 7] and atomistic anisotropy [7]. Since the latter effect is expected to produce FSS values of less than 10 μeV, we conclude that in our case the major contribution is the dot shape anisotropy. This is confirmed by AFM measurements which establish that the openings of the shallow holes are anisotropic with diameter along [1–10] direction being about 1.5 times larger than along [110] (Fig. 1c).

Regarding the trend of our data in Fig. 4a, over a wide range of peak energies (QD sizes) the values of the FSS are nearly constant. In contrast, similar experiments on InAs QDs yield a strong decrease of the FSS from 500 μeV at $E = 1.05$ eV down to -80 μeV at $E = 1.33$ eV [7]. The large FSS versus size effect in InAs QDs is probably related to the additional influence of strain in that material system. For strain-free droplet epitaxial (DE) GaAs QDs, also a decrease of the FSS with dot size is reported [15]. However, the decrease is smaller than for the InAs QDs and the FSS values range from 90 μeV at $E = 1.72$ eV down to 18 μeV at 1.89 eV. The authors explain the

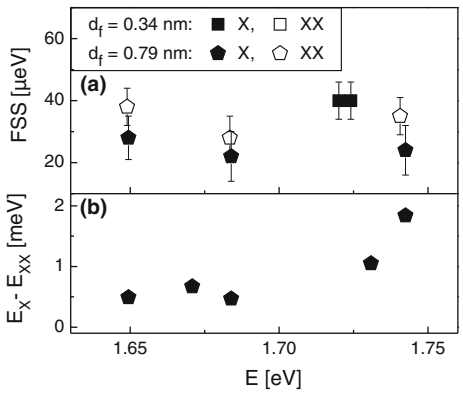

Fig. 4 **a** Neutral exciton *X* and biexciton *XX* fine-structure splitting (FSS) for several shallow-hole GaAs QDs as function of the average peak energy. Two samples were analyzed with different filling levels d_f as indicated. **b** Difference between *X* and *XX* peak maxima for the sample with $d_f = 0.79$ nm. *Error bars* in (**b**) are smaller than the data points

influence of dot size on the FSS with a size-dependent dot shape. A reduction in the QD asymmetry is found when the size is reduced. The present LDE dots are in average larger than the DE dots. We associate our observation of an only negligible influence of dot size on FSS to the shape of the LDE QDs which here does not vary with size.

Finally, Fig. 4b illustrates that the separation between the exciton and biexciton peaks increases with increasing peak energy (decreasing QD size). The exciton binding energy is given by the electron-hole-binding state, whereas the biexciton-binding energy reflects in addition electron–electron and hole–hole interactions. This complex interplay depends sensitively on details of the QD morphology [7]. QDs with low exciton–biexciton splitting are highly interesting since they represent a novel path for entangled photon generation using the time reordering scheme [26].

Conclusions

In conclusion, we have studied a novel type of strain-free GaAs quantum dots which are fabricated by filling of self-assembled nanoholes generated by local droplet etching. Using appropriate process conditions, the resulting QDs have either a very narrow or a broad size distribution which allows to study the single-dot excitonic fine structure over a wide range of QD sizes. The experiments establish sharp excitonic lines for both shallow-hole and deep-hole QDs. For shallow-hole QDs, the measurements reveal values of the fine-structure splitting of 22–40 μeV that do not significantly depend on QD size. In addition, we find a decrease in the exciton–biexciton separation with increasing dot size.

Acknowledgments The authors would like to thank the "Deutsche Forschungsgemeinschaft" for financial support via GrK 1286 and HA 2042/6-1.

References

1. E. Knill, R. Laflamme, G.J. Milburn, Nature **409**, 46 (2001)
2. P. Michler, A. Kiraz, C. Becher, W.V. Schoenfeld, P.M. Petroff, L. Zhang, E. Hu, A. Imamoglu, Science **290**, 2282 (2000)
3. O. Benson, C. Santori, M. Pelton, Y. Yamamoto, Phys. Rev. Lett. **84**, 2513 (2000)
4. A.J. Shields, Nat. Photonics **1**, 215 (2007)
5. M. Bayer, G. Ortner, O. Stern, A. Kuther, A.A. Gorbunov, A. Forchel, P. Hawrylak, S. Fafard, K. Hinzer, T.L. Reinecke, S.N. Walck, J.P. Reithmaier, F. Klopf, F. Schäfer, Phys. Rev. B **65**, 195315 (2002)
6. G. Bester, S. Nair, A. Zunger, Phys. Rev. B **67**, 161306 (2003)
7. R. Seguin, A. Schliwa, S. Rodt, K. Pötschke, U.W. Pohl, D. Bimberg, Phys. Rev. Lett. **95**, 257401 (2005)
8. D. Gammon, E.S. Snow, B.V. Shanabrook, D.S. Katzer, D. Park, Phys. Rev. Lett. **76**, 3005 (1996)
9. M. Bayer, A. Kuther, A. Forchel, A.A. Gorbunov, V.B. Timofeev, F. Schäfer, J.P. Reithmaier, Phys. Rev. Lett. **82**, 1748 (1999)
10. J.J. Finley, D.J. Mowbray, M.S. Skolnick, A.D. Ashmore, C. Baker, A.F.G. Monte, M. Hopkinson, Phys. Rev. B **66**, 153316 (2002)
11. K. Kowalik, O. Krebs, A. Lemaitre, S. Laurent, P. Senellart, P. Voisin, J.A. Gaj, Appl. Phys. Lett. **86**, 041907 (2005)
12. P.B. Joyce, T.J. Krzyzewski, G.R. Bell, B.A. Joyce, T.S. Jones, Phys. Rev. B **58**, R15981 (1998)
13. Ch. Heyn, Phys. Rev. B **64**, 165306 (2001)
14. K. Zhang, Ch. Heyn, W. Hansen, T. Schmidt, J. Falta, Appl. Phys. Lett. **77**, 1295 (2000)
15. M. Abbarchi, C.A. Mastrandrea, T. Kuroda, T. Mano, K. Sakoda, N. Koguchi, S. Sanguinetti, A. Vinattieri, M. Gurioli, Phys. Rev. B **78**, 125321 (2008)
16. S. Kiravittaya, M. Benyoucef, R. Zapf-Gottwick, A. Rastelli, O.G. Schmidt, Appl. Phys. Lett. **89**, 233102 (2006)
17. L. Wang, V. Krapek, F. Ding, F. Horton, A. Schliwa, D. Bimberg, A. Rastelli, O.G. Schmidt, Phys. Rev. B **80**, 085309 (2009)
18. Zh.M. Wang, B.L. Liang, K.A. Sablon, G.J. Salamo, Appl. Phys. Lett. **90**, 113120 (2007)
19. A. Stemmann, Ch. Heyn, T. Köppen, T. Kipp, W. Hansen, Appl. Phys. Lett. **93**, 123108 (2008)
20. Ch. Heyn, A. Stemmann, W. Hansen, J. Cryst. Growth **311**, 1839 (2009)
21. Ch. Heyn, A. Stemmann, R. Eiselt, W. Hansen, J. Appl. Phys. **105**, 054316 (2009)
22. Ch. Heyn, A. Stemmann, W. Hansen, Appl. Phys. Lett. **95**, 173110 (2009)
23. A. Stemmann, Ch. Heyn, W. Hansen, J. Appl. Phys. **106**, 064315 (2009)
24. Ch. Heyn, A. Stemmann, T. Köppen, Ch. Strelow, T. Kipp, M. Grave , S. Mendach, W. Hansen, Nanoscale Res. Lett. **5**, 576 (2010)
25. Ch. Heyn, A. Stemmann, T. Köppen, Ch. Strelow, T. Kipp, S. Mendach, W. Hansen, Appl. Phys. Lett. **94**, 183113 (2009)
26. J.E. Avron, G. Bisker, D. Gershoni, N.H. Lindner, E.A. Meirom, R.J. Warburton, Phys. Rev. Lett. **103**, 048902 (2009)